Geoderma 376 (2020) 114550

Contents lists available at ScienceDirect

Geoderma

journal homepage: www.elsevier.com/locate/geoderma

Phosphorus in 2D: Spatially resolved P speciation in two Swedish forest soils as influenced by apatite weathering and podzolization

Gbotemi A. Adediran[a], J.R. Marius Tuyishime[a], Delphine Vantelon[b], Wantana Klysubun[c], Jon Petter Gustafsson[a,d,*]

[a] Department of Soil and Environment, Swedish University of Agricultural Sciences, Box 7014, 750 07 Uppsala, Sweden
[b] Synchrotron SOLEIL, L'Orme des Merisiers, Saint Aubin BP 48, 91192 Gif-sur-Yvette Cedex, France
[c] Synchrotron Light Research Institute, 111 Moo 6, Suranaree, Muang, Nakhon Ratchasima, Thailand
[d] Department of Sustainable Development, Environmental Science and Engineering, KTH Royal Institute of Technology, Teknikringen 10B, 100 44 Stockholm, Sweden

ARTICLE INFO

Handling Editor: David Laird

Keywords:
Phosphorus retention and speciation
Postglacial forest soils
Apatite weathering
Podzolization
X-ray fluorescence microscopy and spectroscopy

ABSTRACT

The cycling and long-term supply of phosphorus (P) in soils are of global environmental and agricultural concern. To advance the knowledge, a detailed understanding of both the vertical and lateral variation of P chemical speciation and retention mechanism(s) is required, a knowledge that is limited in postglacial forest soils. We combined the use of synchrotron X-ray fluorescence microscopy with multi-elemental co-localisation analysis and P K-edge XANES spectroscopy to reveal critical chemical and structural soil properties. We established a two-dimensional (2D) imagery of P retention and speciation at a microscale spatial resolution in two forest soil profiles formed in glaciofluvial and wave-washed sand. The abundance and speciation of P in the upper 40 cm was found to be influenced by soil weathering and podzolization, leading to spatial variability in P speciation on the microscale (< 200 μm) with P existing predominantly as organic P and as PO_4 adsorbed to allophane and ferrihydrite, according to XANES spectroscopy. These species were mostly retained at sharp edges and in pore spaces within Al and Si-bearing particles. Despite the relatively young age (< 15,000 years) of the soils, our results show primary mineral apatite to have weathered from the surface horizons. In the C horizon however, a large fraction of the P was in the form of apatite, which appeared as widely dispersed (> 600 μm) hot spots of inclusions in aluminosilicates or as discrete micro-sized apatite grains. The subsoil apatite represents a pool of P that trees can potentially acquire and thus add to the biogeochemically active P pool in temperate forest soils.

1. Introduction

Phosphorus (P) is a macronutrient needed for the sustenance of all forms of life on Earth. However, the global supply of P is limited (Cordell et al., 2009; Van Vuuren et al., 2010). Temperate and boreal forest ecosystems in northern Europe are associated with soils that were formed after the last glaciation 8000–15,000 years ago. Most of these were developed in glacial till and glaciofluvial or wave-washed sand (Werner et al., 2017a). The primary production of these ecosystems is usually limited by the availability of nitrogen (N), and currently there are few indications of P limitation (Akselsson et al., 2008; Binkley and Högberg, 2016). However, the increased atmospheric N deposition in the last decades have rendered some forest ecosystems more N-enriched, which may increase problems with N leaching (Gundersen et al., 2006), and thereby make P a more critical nutrient (Yu et al., 2018). In addition, today's forest management methods, with harvesting of biomass, could lead to a successive depletion of bioavailable P in forest soils. This is particularly the case as concerns whole-tree harvesting, but also stem harvesting leads to P losses. A mass balance study carried out for 14,550 Swedish sites revealed that the annual losses of P from forestry exceed 1 kg P ha^{-1} in the southern part of Sweden (Akselsson et al., 2008). This could also contribute to a successive transition from N to P limitation in northern European ecosystems.

The bioavailability of P for plant use depends on its chemical speciation, its relationship with soil particles and proximity to plant roots (Frossard et al., 2000). For P to be bioavailable, it will first need to be weathered from primary minerals, predominantly apatite (Wallander et al., 1997). As many northern European forest soils is of relatively recent origin, they are expected to contain appreciable amounts of apatite in the mineral soil (Walker and Syers, 1976). Apatite weathering has been shown to be strongly dependent on the acidity of the soil; possibly, soil organisms can speed up weathering by excreting organic

* Corresponding author at: Department of Soil and Environment, Swedish University of Agricultural Sciences, Box 7014, 750 07 Uppsala, Sweden.
E-mail addresses: gbotemi.adediran@slu.se (G.A. Adediran), jon-petter.gustafsson@slu.se (J.P. Gustafsson).

https://doi.org/10.1016/j.geoderma.2020.114550
Received 30 March 2020; Received in revised form 13 June 2020; Accepted 17 June 2020
Available online 25 June 2020

acids (Smits et al., 2014; Wallander et al., 1997). Once apatite is dissolved, the released P is potentially bioavailable. However, the released orthophosphate (*o*-phosphate ions) may also be adsorbed by iron (Fe) and aluminium (Al) (hydr)oxides including allophane, which are ubiquitous weathering products in the B horizons of Spodosols (Gustafsson et al., 1999). In addition, some P is also stored in soil organic matter in a variety of P forms (Vincent et al., 2012).

The bulk chemical speciation of P in a soil sample can be estimated by P K-edge XANES spectroscopy with linear combination fitting (Beauchemin et al., 2003). There are many recent examples on the successful use of this technique, also for forest soils (Prietzel et al., 2016). Although the bulk speciation of P is useful to know, it is important to remember that the spectra obtained represent an average of a large number of P phases present in a sample. This can make individual assignments, based on linear combination fitting, uncertain (Gustafsson et al., 2020). In addition, the bulk speciation is not necessarily related to bioavailability, as it does not indicate to what extent the P phases are geochemically active and/or available for plant uptake.

The use of synchrotron-based X-ray fluorescence (μ-XRF) microscopy in combination with spotwise P K-edge X-ray atomic absorption near-edge structure (μ-XANES) spectroscopy can offer valuable additional information on P speciation as it allows multi-elemental mapping as well as solid-state P speciation analysis in-situ (Baumann et al., 2019; Rivard et al., 2016; Werner et al., 2017b). For example, Rivard et al. (2016), studying the effects of fertilization on P species in agricultural soils from Illinois, noticed the presence of some “hot spots” with an enrichment of Ca-bound P, probably apatite. However, their effect on the bulk XANES spectra were insignificant. Werner et al. (2017b), who studied a group of Bavarian Cambisols, found that P-enriched areas coincided with the presence of Al and Fe hydrous oxides, showing that P was bound mainly to Al and Fe of these phases. In microsites, they also found indications of the presence of Al phosphates and also of unusual magnesium (Mg) phases such as $MgHPO_4$, which could not be identified with bulk P-XANES methods. Hesterberg et al. (2017) collected P K-edge XANES spectra from 12 microsites of one Histosol soil sample. In all microsites the P was dominated by organic P and Al-bound P, but the relative proportions of the different species were variable, confirming that μ-XANES was able to provide additional information on the P speciation in localized areas of the samples.

Moreover, bulk soil P-XANES spectroscopy has been used to elucidate weathering-induced apatite dissolution from which the P released can be transformed to other species, such as organic P and P adsorbed on Fe and Al (hydr)oxides, or leached (Eriksson et al., 2016; Prietzel et al., 2016). As a result, the apatite concentration increased with soil depth while the concentrations of organic P and adsorbed P species decreased with depth. This observation is consistent also with previous studies that relied on results from wet extractions (Walker and Syers, 1976; Frossard et al., 1989). However, electron microscopy has been used to show small amounts of apatitic P to be preserved as ‘mineral apatite inclusions’ (a mineral species present within the matrix of another mineral species) in slowly weathered silicates (Heindel et al., 2018; Syers et al., 1967).

Despite these research efforts, there are many aspects of the two-dimensional (2D) spatial distribution of P that remain unclear, and what this means for our interpretation of soil P cycling and weathering phenomena. Moreover, there is no study to date which has established a 2D-imagery of P distribution and chemical speciation as a function of depth in a soil profile. This visualisation is critical for the accurate conceptualisation of molecular-scale chemical and physical reactions of P in soils and such knowledge is fundamental to the understanding of how P speciation changes over time in response to soil-forming processes (Prietzel et al., 2016; Werner et al., 2017b).

The current study capitalises on recent advances in synchrotron based micro-focused-X-ray fluorescence microscopy and spectroscopy to acquire images of multi-elemental distributions, grain architecture, pore space distributions, and the vertical and lateral distribution of P chemical species at a very high (< 3 μm) spatial resolution.

The specific aim is to comprehensively study two forest soil profiles in order to: (i) establish the effects of postglacial weathering on the spatial abundance and distribution of primary apatite, (ii) reveal the predominant chemical species of P under the acidic soil conditions that prevail in Podzols, and (iii) elucidate the mechanisms that govern both the vertical and lateral retention of P, at the microscale.

2. Methodology

2.1. Soil sampling and sample preparation

Two soil profiles were excavated in coniferous forests at Tärnsjö and Tönnersjöheden, Sweden, respectively (coordinates: 60.14°N 16.92°E and 56,42°N 13.40°E). The predominant vegetation was *Pinus sylvestris* and *Picea abies* of about 70–120 years of age (Gustafsson et al., 2015; Zetterberg et al., 2013). The soils at the two sites were formed under temperate climate. While the soil at Tärnsjö was formed in wave-washed sand and classified as an Albic Podzol (IUSS Working Group WRB, 2014), the soil at Tönnersjöheden was developed in sandy glaciofluvial material. Although podzolized, it did not classify as a Podzol due to significant mixing of the upper horizons and was therefore classified as Dystric Arenosol (Hansson et al., 2011; IUSS Working Group WRB, 2014). At Tärnsjö, an eluvial (E) horizon of about 2 cm thick was found under the organic layer (0–2 cm in depth). This was sampled as well as the uppermost Bs horizon at 2–10 cm. Other mineral soil samples thereafter were sampled at 10 cm intervals to a depth of 100 cm. As there was no E horizon in the profile at Tönnersjöheden, only an A horizon with a gradual transition to the underlying B horizon, the soil samples were collected at 10 cm intervals from the top (A horizon) to a depth of 100 cm. Soils for micro-focused X-ray microscopy and spectroscopy were gently sieved (< 5 mm) to remove stones and debris before air-drying for 72 h. Representative samples from each depth were then embedded in high-purity epoxy resin. Micro-polished petrographic thin sections of 30 μm thick were prepared at TS Lab & Geoservices snc, Cascina, Italy. Soil samples for other analysis were dried at 60 °C for 48 h and subsequently sieved (< 2 mm).

2.2. Measurements of selected soil chemical properties

On sieved (< 2 mm) soil samples, the pH value was measured in a deionised water suspension with a glass electrode (soil: solution ratio 1:2.5). Total P contents (P-t) were determined after microwave-assisted digestion in sealed teflon vessels with a 10:1 mixture of concentrated HNO_3:H_2O_2 and subsequent measurement by inductively coupled plasma sector field mass spectrometry (Church et al., 2017). The soils were also subjected to extraction with 0.2 M oxalate buffer at pH 3.0 to quantify non-crystalline and organically-bound metals using the method of van Reeuwijk (1995). The concentrations of P, Al and Fe (designated as P-ox, Al-ox and Fe-ox respectively) in the extract were analyzed by inductively coupled plasma optical emission spectroscopy (ICP-OES) using a Thermo Scientific Icap 6000 instrument (Thermo Fisher Scientific, Waltham, MA, USA). The concentration of inorganic P in the oxalate extract (PO_4-ox) was determined using a Seal AA3 Autoanalyzer (Seal Analytical GmBH, Norderstedt, Germany) employing the acid molybdate method as modified by Wolf and Baker (1990). The concentration of oxalate-extractable organic P (OrgP-ox) was estimated by subtracting PO_4-ox from P-ox. Organic carbon (C) and total nitrogen (N) were analysed by dry combustion (CHN600, LECO).

2.3. P speciation by bulk soil P K-edge XANES analysis

Bulk P K-edge XANES spectra were collected on the soil samples at beam line BL8 of the Synchrotron Light Research Institute (SLRI) in Nakhon Ratchasima, Thailand (Klysubun et al., 2020). Prior to bulk XANES analysis, ~ 4 g of soil samples were milled and sieved

through < 0.05 mm to minimize self-absorption. Powdered samples were then packed into 2 mm thick stainless steel holders (1 × 1.5 cm with a sample window of 0.5 × 1 cm) and covered with polypropylene film (Eriksson et al., 2016). The beamline was equipped with an InSb (1 1 1) crystal monochromator and a solid state 13-element Ge fluorescence detector. The beam size was 12.5 × 0.9 mm and beam flux was 2×10^{11} photons s^{-1} (100 mA)$^{-1}$. To minimize X-ray absorption by air, the sample compartment was filled with helium gas. Spectra of samples and standards were recorded across an energy range from 2100 to 2320 eV. The step size was 2 eV between 2100 and 2132 eV, 1 eV between 2132 and 2144 eV, 0.2 eV between 2144 and 2153 eV, 0.3 eV between 2153 and 2182 eV, and 5 eV between 2182 and 2320 eV. All measurements were recorded using a dwell time of 3 s per energy step.

2.4. Synchrotron micro-focused μ-XRF and μ-XANES

The petrographic soil sections were subjected to both μ-XRF imaging and μ-XANES analysis at the X-ray microscopy beamline LUCIA of the French national synchrotron research facility SOLEIL. The beamline is fitted with a Si(1 1 1) double crystal monochromator. Transmission, fluorescence and total electron yield detection were made simultaneously by means of a silicon pin diode, a silicon drift diode and a measurement of the drain current, respectively (Vantelon et al., 2016). Focusing of the X-ray beam (2.5 × 2.5 μm) was performed with two Kirkpatrick-Baez (K-B) mirrors system. The photon flux was 6×10^{11} photons s^{-1} at 2.6 keV. To minimize X-ray absorption by air, the analysis was performed in a vacuum environment.

Considering the low concentration of P in our thin-sectioned samples and the need to obtain high quality P K-edge μ-XANES spectra, the beamline was optimized for low energy mapping at microscale resolution, and μ-XRF images (600 × 600 μm) of Na, Mg, Al, Si and P were acquired with a dwell time of 0.3 s using a step size of 3 × 3 μm. Although at this low energy we were unable to utilize μ-XRF microscopy to obtain information about the interactions of P with important elements such as Ca and Fe, it was possible to use unique features of the μ-XANES spectra to identify P species associated with Ca and Fe as well as with organic P. For example, calcium phosphates show post-edge shoulders that are unique for different calcium phosphate minerals, Fe bound P shows a distinct pre-edge peak, and organic-P species have a broad white line peak displaced towards lower energy (Hesterberg, 2010; Gustafsson et al. 2020) (see supplementary material Fig. S1).

Spot-wise μ-XANES of P was therefore performed with respect to the spatial distribution of P as revealed by μ-XRF. The P spots were chosen at soil particle surfaces and at pore spaces across the maps to reflect as much as possible the heterogeneity in P distribution that was revealed by μ-XRF. The P K-edge μ-XANES spectra were recorded in fluorescence mode across an energy range from 2100 to 2320 eV. The step size was 2 eV between 2100 and 2139 eV, 1 eV between 2140 and 2146 eV, 0.2 eV between 2146 and 2160 eV, 0.3 eV between 2160 and 2190 and 5 eV between 2195 and 2320 eV. All XANES measurements were recorded using a dwell time of 3 s per energy step. At every selected spot, 4 to 5 high quality μ-XANES scans were acquired and merged to represent a spot.

μ-XRF mapping were also performed on selected P standards and high quality micro-focused P K-edge XANES spectra were obtained at P hot spots. These standards include hydroxyapatite, PO_4 adsorbed to ferrihydrite, variscite, PO_4 adsorbed to aluminum hydroxide, PO_4 adsorbed to allophane and natural soil organic phosphorus from forest mor (SOP). These were complemented with bulk P K-edge spectra of other P compounds such as natural apatite (from Taiba, Sudan), amorphous calcium phosphate, iron(III) phosphate, PO_4 adsorbed to goethite, aluminum phosphate and PO_4 adsorbed to gibbsite. These standards were collected at BL8 of SLRI and are part of our database of P standards used for routine P speciation analysis in soil. The sources and preparation of the standards are described in Gustafsson et al. (2020). Together, these compounds represent the major P associations (i.e., Ca-P, Fe-P, Al-P, P adsorbed to Fe and Al, and organic P) that are often encountered in soils.

2.5. Analysis of X-ray fluorescence and X-ray absorption data

The μ-XRF spectra were dead-time corrected and normalized to incoming beam intensities before individual elemental spectra deconvolution. Microscale-resolution elemental maps were obtained after fitting each pixel μ-XRF spectrum using the PyMca X-ray Fluorescence Toolkit (Solé et al., 2007). The ATHENA software package was used to subtract the background and normalize all μ-XANES and bulk soil P XANES spectra (Ravel and Newville, 2005). Solid-phase P speciation was estimated by linear combination fitting (LCF) analysis (Eriksson et al., 2016; Tannazi and Bunker, 2005) using weighted combinations of the reference spectra (Fig. S1). No energy shifts were permitted in the fitting procedure and the fit combinatorics were not forced to sum to 100%. A maximum of 4 out of 15 standard compounds were allowed during the LCF using a least-squares algorithm of the sample XANES spectrum from 2144.05 to 2184.05 eV. The goodness of the fit was estimated by calculating the R factor of the fit; $R = \Sigma_i$ (experimental − fit)$^2/\Sigma_i$ (experimental)^2 (Ravel and Newville, 2005). The sums (Σ) were over 142 data points as flattened mu (E). A lower R factor represents a better match between the standard spectra and the sample spectrum. For the bulk P K-edge XANES results from SLRI, standard deviations of the weights were calculated with a Monte-Carlo approach, in which uncertainties in energy calibration and normalization were considered (for a full account, see Gustafsson et al., 2020). However, for the μ-XANES data, information on these uncertainties were not available, and instead the standard deviations were those given by Athena, which consider only uncertainties of the LCF method itself (Ravel and Newville, 2005).

3. Results

3.1. Soil characteristics

Selected soil chemical properties are presented in Table 1. The soils were predominantly acidic. The lowest pH at both sites was in the organic layer and in the uppermost mineral soils. In Tärnsjö, the pH increased from 4.0 in the organic layer to 6.2 at 80 cm depth before decreasing slightly to between 5.8 and 6.0 at the bottom of the profile. In Tönnersjöheden, the pH increased from 3.7 in the organic layer to 4.6 at 20 cm depth and then remained stable at between pH 4.7 and 4.8 from 30 cm to the bottom of the profile. Total P (P-t) in the mineral soils ranged from 2 to 20 mmol kg^{-1}. In Tärnsjö, the lowest amount of P-t was observed at the E horizon (0–2 cm) while the highest amount was in the illuvial Bs horizon (10–20 cm). A similar pattern was observed in Tönnersjöheden with the lowest amount of P-t at the A horizon (0–10 cm) and the highest at the B horizons (20–50 cm). The distribution of oxalate-extractable elements in the two profiles exhibited similar trends, which were similar to those seen in previous studies on Swedish Podzols (Bain et al., 2003). For example in Tärnsjö, the lowest concentrations of P-ox, Al-ox and Si-ox were in the E horizon, whereas they reached a maximum in the Bs horizon with concentrations of 19, 166 and 31 mmol kg^{-1} respectively before decreasing with depth. The Fe-ox concentrations showed a similar pattern with the lowest concentration in the E horizon and the maximum concentrations of 64 mmol kg^{-1} in the Bs horizon. The Fe-ox concentration also decreased with depth to a concentration of 6.3 mmol kg^{-1} at 70–80 cm but further down it increased again to between 18.7 and 25.2 mmol kg^{-1} at 80–100 cm depth. Similarly, the concentrations of P-ox, Al-ox and Si-ox were lowest in the A horizon of Tönnersjöheden and had maximum concentrations in the Bs horizons (10–30 cm) before decreasing with depth. The amount of Fe-ox in the Tönnersjöheden profile was highest already in the A horizon and then decreased with depth. While most of the P-ox was organic in the uppermost two

Table 1
Soil pH, concentrations (mmol kg^{-1}) of total P (P-t), oxalate (ox) extractable – P (P-ox), phosphate (PO_4-ox), organic P (OrgP-ox), Fe (Fe-ox), Al (Al-ox), Si (Si-ox) and percentage organic carbon (Org-C) and total nitrogen (Total-N) in Tärnsjö and Tönnersjöheden soil profile.

Horizon/Depth (cm)	pH	P-t	P-ox	PO_4-ox	OrgP-ox	Fe-ox	Al-ox	Si-ox	Org-C	Total-N
		mmol kg^{-1}								(%)
Tärnsjö										
Oe Mor	4.0	18.4	4.3	2.6	1.7	8.9	25.3	0.5	46.66	1.24
E 0–2	4.3	2.0	0.5	0.2	0.3	4.2	10.4	0.4	0.84	0.02
Bs 2–10	4.6	15.0	10.7	9.4	1.3	54.2	84.2	10.8	1.29	0.04
10–20	4.9	20.9	19.9	17.0	2.9	64.2	166.5	31.7	1.08	0.03
20–30	5.2	15.3	10.9	10.0	0.9	29.6	111.9	24.7	0.32	0.01
BC 30–40	5.4	10.7	5.0	4.3	0.7	10.3	54.5	16.2	0.13	< 0.005
C 40–50	5.7	11.8	3.8	3.3	0.5	6.8	42.0	16.8	0.07	< 0.005
50–60	5.9	12.1	3.8	3.3	0.5	9.8	40.2	14.3	0.06	< 0.005
60–70	6.1	15.9	2.8	2.4	0.4	7.2	28.5	13.2	0.04	< 0.005
70–80	6.2	16.0	2.1	1.7	0.4	6.3	23.8	11.1	0.04	< 0.005
80–90	6.0	15.0	2.2	1.7	0.5	25.2	25.3	12.1	0.07	< 0.005
90–100	5.8	17.2	3.0	2.3	0.7	18.7	27.8	12.5	0.06	< 0.005
Tönnersjöheden										
Oe Mor	3.7	21.6	5.5	2.1	3.4	13.8	26.2	0.6	44.80	1.47
A 0–10	4.2	8.3	5.6	2.0	3.6	131.7	98.7	2.7	4.00	0.16
Bs 10–20	4.6	14.2	11.2	6.7	4.5	125.4	318.9	53.8	3.03	0.14
20–30	4.7	17.5	13.2	10.0	3.2	82.9	280.7	57.4	1.66	0.08
30–40	4.8	18	14.1	10.6	3.5	64.3	270.3	55.0	1.38	0.07
40–50	4.7	18	11.6	9.0	2.6	57.2	172.4	32.1	1.21	0.05
50–60	4.7	16.8	10.6	8.1	2.5	53.8	139.9	23.4	1.00	0.04
BC 60–70	4.8	12.8	7.7	5.6	2.1	25.0	104.5	20.1	0.79	0.03
C 70–80	4.8	14.9	6.8	5.0	1.8	14.8	75.4	15.1	0.55	0.02
80–90	4.8	16	6.3	4.9	1.4	11.6	61.4	13.2	0.34	0.01
90–100	4.8	12.5	6.6	5.0	1.6	18.7	72.2	13.7	0.47	0.02

horizons at both sites, P-ox was dominated by inorganic PO_4 deeper down in the mineral soil (i.e. throughout the B and C horizons), particularly in the Tärnsjö soil, which had a relatively low organic C content in the B horizon (Table 1).

3.2. P speciation by bulk soil P K-edge XANES

Linear combination fit results of bulk P K-edge XANES spectra are reported in Fig. 1. They showed a predominance of organic P in the O horizon, Al- and Fe-bound P in the A and B horizons, and the presence of primary mineral apatite in the C horizons of the two soil profiles. It is worthy of note that the Ca-bound P was detectable by bulk P K-edge XANES from 20 to 30 cm soil depth, with the abundance appearing to increase with depth at both sites.

3.3. 2D imagery of soil architecture with respect to P retention and speciation

As expected in soils formed on siliceous parent materials, μ-XRF imaging revealed Si and Al as the main constituents of the soil grains (Fig. S2-S3). A morphological analysis of the spatial variation and co-localisation of Si and Al was therefore deemed sufficient to depict particles and pore space distribution in the soil profiles. 2D tri-colour co-localisation of Si (red), Al (blue) and P (green) were therefore used to re-construct the spatial retention of P species with respect to soil particles and pore-spaces distributions across the soil profiles (Fig. 2). The results of this micro-spectroscopic analysis is described below.

(i) P retention and speciation at the E horizon

In agreement with the results of P chemical extractions, synchrotron μ-XRF imaging showed the lowest P abundance in the E horizon (0–2 cm depth) of the Tärnsjö profile (Fig. 2a). The P concentration was too low to yield P K-edge XANES spectra (both by micro and bulk powdered XANES) that could be analysed to deduce the chemical speciation of P. However, morphological examination showed most of the P to be retained at the surface/within the cracks of microscale (< 20 μm sizes) Si (mostly devoid of Al) containing grains (Fig. S4).

(ii) P retention and speciation at the A and B horizons

A morphological examination of soil grains at the A horizon in Tönnersjöheden (0–10 cm) and the uppermost B horizon in Tärnsjö (2–10 cm) showed that the majority of the soil grains contained both Si and Al (purple colour) (Fig. 2a-b). Phosphorus (P, green) at these depths was mostly retained at the edges and within pore spaces of the soil particles. It is worthy of note that the edges of the non-Al-bearing (mainly silica) particles appeared to contain some P. Moreover, P appeared also to be retained within the cracks that were probably created by soil weathering at the surface of the largest grain in the Tärnsjö 2–10 cm sample. Furthermore, results of spot-wise P speciation analysis by μ-XANES showed significant spatial heterogeneity within the soil grains at the microscale. For example, while P in point (a) of Tärnsjö 2–10 cm existed predominantly as Fe-bound P (e.g. ferrihydrite-bound PO_4), there was a different P speciation in point (b), where P was instead present as Al-bound P (e.g. allophane-bound PO_4) (Table 2, Fig. S5).

The spatial variation in chemical speciation is easily seen when examining the differences in the pre-edge peaks of the P K-edge XANES spectra (Fig. S5), despite the two spots being < 200 μm apart (Fig. 2). Pronounced pre-edge peaks that occur between 2,149 and 2,152 eV are typical for Fe-associated P, while the pre-edge resonances for Al-bound P are much smaller (Hesterberg et al., 1999). Similar microscale heterogeneity in P speciation was observed in Tönnersjöheden 0–10 cm. For example, while P at point (c) of this depth existed predominantly (56 ± 3% of total P) as Fe-P there was no Fe-P at point (e) which existed predominately (70 ± 6% of total P) as Al-P (Table 3, Fig. S6). The content of organic P as assessed by P K-edge XANES ranged from 9 ± 2 to 19 ± 4% and from 19 ± 1 to 30 ± 3% of total P at Tärnsjö 2–10 cm and Tönnersjöheden 0–10 cm, respectively. In both samples, organic P as assessed by P K-edge XANES was on average < 25 ± 3% of total P, while Al and Fe-bound P were the predominant (up to 75 ± 8%) P species, which were found at the edges and pore spaces of the soil grains.

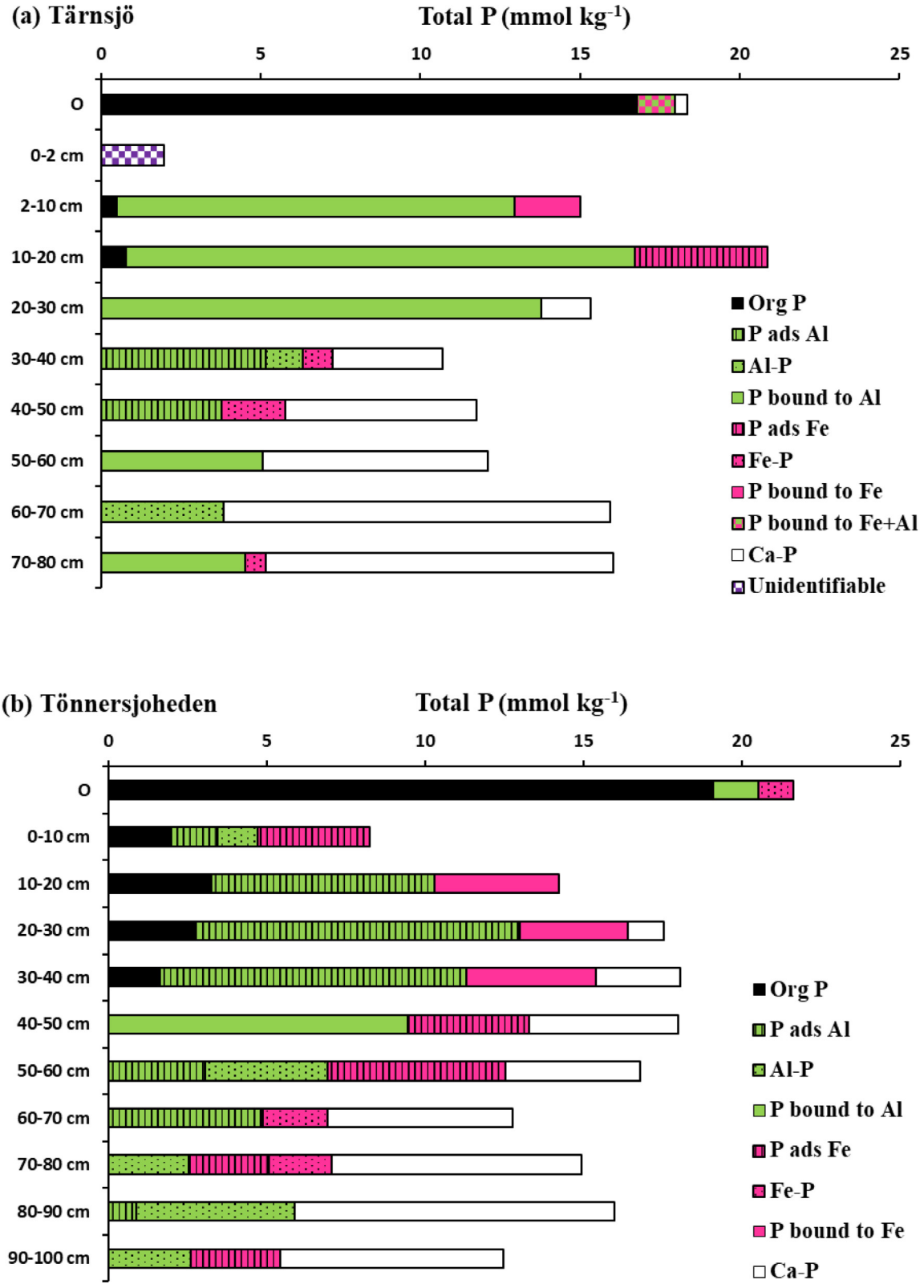

Fig. 1. Phosphorus speciation in the (a) Tärnsjö and (b) Tönnersjöheden soil profiles as evidenced from linear combination fitting (LCF) of bulk soil P K-edge XANES spectra. P ads Al and P ads Fe refer to PO_4 adsorbed to Al and Fe minerals (e.g. PO_4 adsorbed to allophane and PO_4 adsorbed to ferrihydrite), respectively. Al-P and Fe-P refer to $AlPO_4$ and $FePO_4$ mineral phases, respectively. P bound to Al and P bound to Fe represent cases when probabilistic LCF analysis could not differentiate between PO_4 adsorbed to Al from $AlPO_4$ minerals and PO_4 adsorbed to Fe from $FePO_4$ minerals, respectively. In the O horizon of Tärnsjö, P bound to Fe + Al is used as probabilistic LCF could not distinguish between P bound to Al and P bound to Fe.

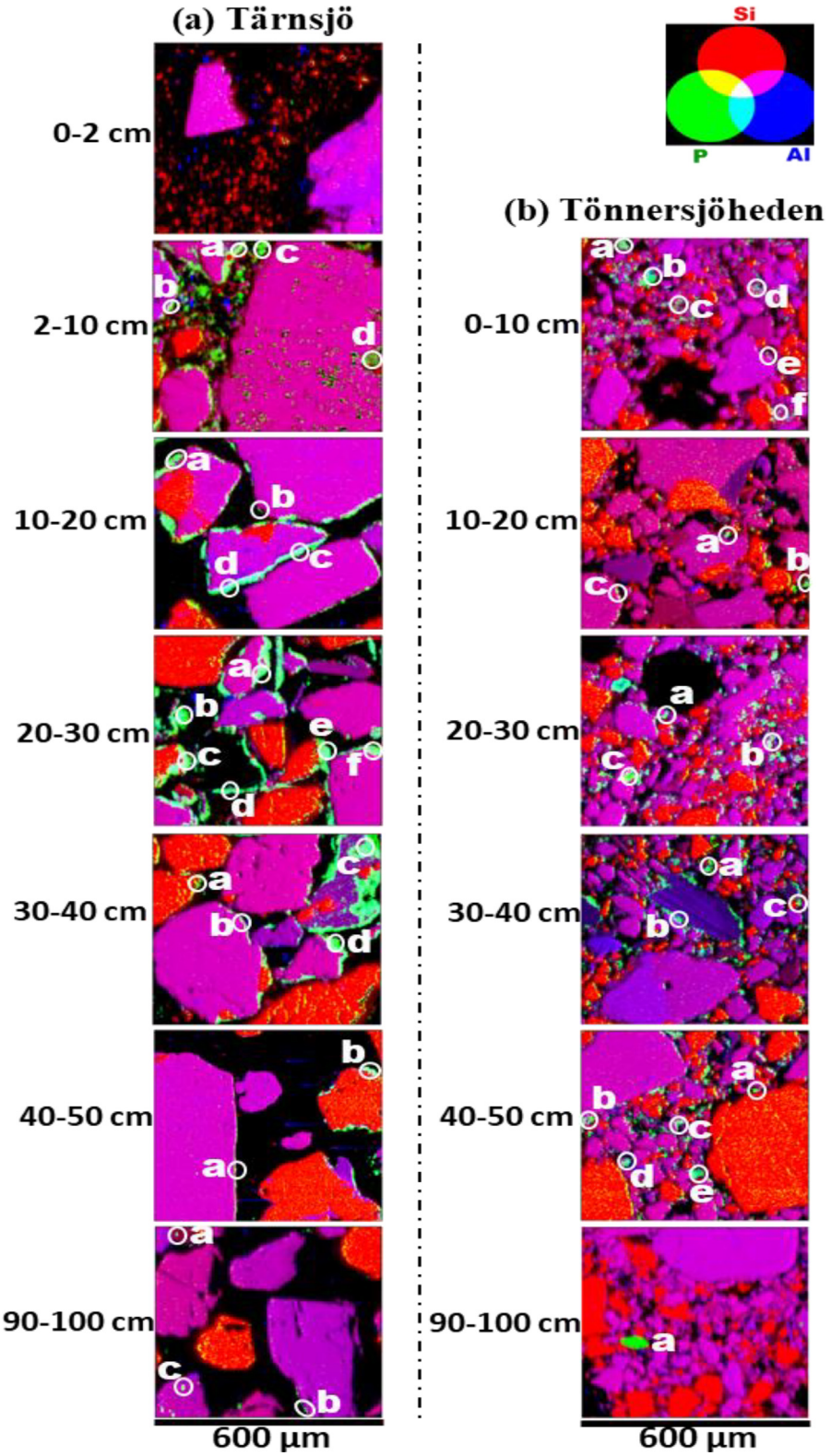

Fig. 2. Spatial variation in P (green) distribution and retention at the edges, surfaces and within pore spaces of Al (blue) and Si (red) bearing soil particles in the (a) Tärnsjö and (b) Tönnersjöheden profiles. The letters a – f on the maps represent spots at which P K-edge μ-XANES data were acquired.

Furthermore, the Tärnsjö 10–20 cm sample contained less of fine (< 20 μm size) particles when compared to the 2–10 cm depth above it. The pore spaces were therefore wider and P was mainly retained at the edges of Si- and Al-bearing particles. The P speciation was also heterogeneous at the microscale. For example, while Fe-bound P was the main form of P at points (a) and (b), P existed predominantly as Al-bound P at points (c) and (d) (Table 2, Fig. S7). The microscale heterogeneity in P speciation was even more pronounced in Tönnersjöheden 10–20 cm (Table 3). For example, while P in point (a) existed predominantly (~90 ± 6%) as inorganic P (as P bound to Fe and Al), in point (b), < 200 μm away, there was a hot spot of organic P (~70 ± 3% of total P at the spot; Fig. S8) according to XANES-LCF.

Table 2
Phosphorus speciation in Tärnsjö soil profile as evidenced from linear combination fitting (LCF) of spot-wise μ-XANES and bulk soil P K-edge XANES spectra. The fits are expressed as percentage contributions from selected P standards. The *R*-factor is a measure of goodness-of-fit = $\Sigma(\text{data} - \text{fit})^2/\Sigma(\text{data})^2$.

Soil profile	μ-XANES Spots	Organic P	Fe bound P		Al bound P		CaP	*R*-factor
			FeP	P adsorbed on Fe	AlP	P adsorbed on Al		
2–10 cm	a	9 ± 2		64 ± 9		27 ± 6		0.0043
Bs	b	13 ± 2		24 ± 7		63 ± 6		0.0028
	c	19 ± 4		35 ± 11		46 ± 8		0.0076
	d	16 ± 2		44 ± 8		40 ± 6		0.0034
	Bulk	3 ± 3		*14 ± 5*[1]		83 ± 6		0.0022
10–20 cm	a	15 ± 2		51 ± 8		34 ± 6		0.004
	b	12 ± 3		49 ± 12		39 ± 9		0.0076
	c			32 ± 2		68 ± 2		0.0009
	d			17 ± 3	15 ± 2	68 ± 3		0.0016
	e	11 ± 2		38 ± 8	22 ± 2	29 ± 6		0.0035
	Bulk	4 ± 4		20 ± 6		*76 ± 8*[1]		0.0012
20–30 cm	a	5 ± 1		34 ± 5	15 ± 2	46 ± 4		0.0012
	b	5 ± 1		29 ± 4		66 ± 3		0.0007
	c			20 ± 2	12 ± 1	68 ± 2		0.0005
	d	6 ± 2		38 ± 6		56 ± 4		0.0015
	e	12 ± 1			8 ± 2	80 ± 2		0.0029
	f	10 ± 1		29 ± 5		61 ± 4		0.0013
	Bulk					*90 ± 4*[1]	10 ± 4	0.0012
30–40 cm	a	16 ± 3		23 ± 8		61 ± 8		0.0059
BC	b			38 ± 2	5 ± 1	57 ± 2		0.0011
	c	5 ± 2		23 ± 9		74 ± 7		0.0038
	d				25 ± 2	75 ± 2		0.002
	Bulk		9 ± 5		11 ± 7	48 ± 3	32 ± 4	0.0021
40–50 cm	a				20 ± 1	80 ± 1		0.0009
C	b	9 ± 1			11 ± 3	80 ± 3		0.0046
	Bulk		17 ± 4			32 ± 2	51 ± 3	0.0023
90–100 cm	a	9 ± 2		25 ± 6		66 ± 5		0.0018
	b	14 ± 2		32 ± 8		54 ± 6		0.0029
	c						100	
	Bulk[2]		4 ± 4			*28 ± 2*[1]	68 ± 3	0.0069

[1] Probabilistic LCF could not differentiate between adsorbed and precipitated species of P bound to Fe or Al.
[2] Bulk soil P K-edge XANES results are shown for the 70–80 cm depth, as results for the 80–100 cm depth were not available. A full data set of bulk soil P K-edge probabilistic LCF is provided under research data.

With increasing depth in the B horizon (down to 40 cm depth), P speciation in the Tärnsjö soil became less heterogeneous as Al- followed by Fe-bound P dominated most of the P microsites (Table 2-3, Fig. S9-S12). The predominance of Al-bound P was in accordance with the greater concentration of oxalate-extractable Al as compared to oxalate-extractable Fe (Table 1).

It cannot be excluded that some of the P that was assigned to ferrihydrite- and allophane-bound PO_4 was adsorbed organic P species such as phytate rather than PO_4 (Prietzel et al., 2016). In the LCF we did not use any standard for adsorbed phytate, as it was shown that the standard for adsorbed phytate to ferrihydrite and allophane could be well described (with an R factor < 0.001) with about 50% organic P and 50% ferrihydrite or allophane (Gustafsson et al, 2020). Thus, the P K-edge XANES technique used here is not well suited to determine the contribution of adsorbed phytate with any confidence. This constitutes a slight uncertainty for the results obtained in the upper B horizons, where there was both organic P and ferrihydrite- and allophane-bound PO_4 according to our results. Nevertheless, the results from the oxalate extraction show that adsorbed phytate is likely only a very minor part of the adsorbed P in the Tärnsjö soil, as the extracted organic P was only a very small fraction of the extracted total P (Table 1). In the Tönnersjöheden soil, adsorbed phytate could be slightly more important, but still of smaller significance than adsorbed PO_4, as evidenced by the relationship between inorganic and organic P in the oxalate extract (Table 1).

(iii) P speciation and retention at upper and lower C horizons

The P speciation in the upper C horizon (40–50 cm depth) showed trends similar to the ones observed at the lower B horizons as P was adsorbed at the edges of soil grains or existed as coatings on the flat surfaces of Si-bearing particles at the two sites. At this depth, P existed mainly as inorganic P in both sites. However, while P at all studied spots in Tärnsjö 40–50 cm exhibited little spatial variability and existed mainly as Al-bound P, the P species at Tönnersjöheden 40–50 cm were more diverse, and they consisted mainly of a mix of Al- and Fe-bound P species at the studied spots (Fig. S13-S14).

At the lowest depth of 90–100 cm, there was significant heterogeneity in P speciation when compared to the upper horizons. In the Tärnsjö 90–100 cm sample, the P in points (a-b) existed predominantly as Al- and Fe-bound P, whereas in point (c) P K-edge μ-XANES detected a hot spot of Ca-bound P, with a XANES spectrum that most resembled apatite (Fig. S15). Detailed morphological examination showed this Ca-bound P spot to be about 10–20 μm in size and to be associated with a larger (> 150 μm) Al and Si-bearing particle, probably a feldspar (Fig. 2a), in which the apatite was present as an inclusion. A similar finding was made at Tönnersjöheden 90–100 cm. Here the Ca-bound P spot appeared as a discrete mineral grain of about 75 μm size (Fig. 2b and Fig. S16). In both cases the P concentration was very high, suggesting the presence of apatite or almost pure apatite.

4. Discussion

4.1. Heterogeneity of P chemical species at soil microsites

Soils are developed through a large number of biogeochemical processes that occur at the same time. In the midst of this complexity, a concise analysis of micrometre-scale chemical speciation within a volume of intact soil sample is fundamental to the understanding of molecular-level chemical reactions that govern the long-term cycling of

Table 3
Phosphorus speciation in the Tönnersjöheden soil profile as evidenced from linear combination fitting (LCF) of spot-wise μ-XANES and bulk soil P K-edge XANES spectra. The fits are expressed as percentage contributions from selected P standards. The *R*-factor is a measure of goodness-of-fit = Σ (data − fit)^2/Σ (data)^2.

Soil profile	μ-XANES Spots	Organic P	Fe bound P		Al bound P		CaP	*R*-factor
			FeP	P adsorbed on Fe	AlP	P adsorbed on Al		
0–10 cm	a	21 ± 1			22 ± 1	21 ± 3		0.0008
A	b	22 ± 1		37 ± 3	19 ± 1	22 ± 3		0.0007
	c	19 ± 1		56 ± 3	17 ± 1	8 ± 2		0.0006
	d	21 ± 2		29 ± 6	36 ± 2	14 ± 4		0.002
	e	30 ± 3			56 ± 3	14 ± 3		0.0069
	f	19 ± 1		27 ± 2	54 ± 2			0.0032
	Bulk	24 ± 5		43 ± 6	15 ± 7	18 ± 3		0.0025
10–20 cm	a	7 ± 1		41 ± 3	18 ± 1	34 ± 2		0.0003
Bs	b	71 ± 3			29 ± 3			0.0321
	c	6 ± 1		15 ± 4	33 ± 2	46 ± 3		0.0009
	Bulk	23 ± 3		*28 ± 8*[1]		49 ± 8		0.0008
20–30 cm	a	9 ± 1		20 ± 5		71 ± 4		0.0011
	b	5 ± 1		32 ± 6		63 ± 4		0.0014
	c			13 ± 2	5 ± 1	82 ± 2		0.0009
	d	10 ± 2		33 ± 6		57 ± 4		0.0017
	Bulk	16 ± 5		*20 ± 8*[1]	6 ± 2	59 ± 8	6 ± 5	0.0007
30–40 cm	a	19 ± 3		15 ± 10		66 ± 7		0.0047
	b	23 ± 3		25 ± 12		52 ± 9		0.0073
	c			33 ± 3	18 ± 1	49 ± 2		0.0013
	Bulk	9 ± 7		*23 ± 9*[1]		54 ± 9	15 ± 4	0.0008
40–50 cm	a	27 ± 2		32 ± 6		41 ± 6		0.0034
	b			39 ± 6		61 ± 3		0.0018
	c			48 ± 5	32 ± 3	20 ± 4		0.0051
	d			50 ± 2		50 ± 2		0.0009
	e	17 ± 2		16 ± 4	20 ± 1	47 ± 3		0.0009
	Bulk			21 ± 7		*53 ± 8*[1]	26 ± 6	0.0008
90–100 cm	a						100	
C	*Bulk*			23 ± 3	21 ± 5		56 ± 3	0.0014

A full data set of bulk soil P K-edge probabilistic LCF is provided under research data.
[1] Probabilistic LCF could not differentiate between adsorbed and precipitated species of P bound to Fe or Al.

elements. Examination of the variation in P chemical species in spots within 600 × 600 μm of intact soil samples revealed spatial heterogeneity in P chemical compositions. However, the extent of this heterogeneity was different depending both on the species and on the soil horizon. In the C horizon at 90–100 cm depth Ca phosphates, predominantly apatite, were important at both sites. The apatite was very probably inherited from the glaciofluvial parent material, and the μ-XANES results show the apatite to occur as grains or inclusions with a locally very high P concentration causing a patch-wise, highly heterogeneous P distribution in the soil. This is in agreement with earlier research in which apatite was identified in glacial till material with electron microscopy (Nezat et al., 2008). There were, however, also signs of weathering effects in the C horizon, as part of the P were bound to Al and Fe in coatings and in pore spaces. Here, most of the P was present as phosphate adsorbed to allophane, and to a minor extent ferrihydrite.

In the more acidic B horizon, the P speciation in both soils was dominated by Al- and Fe-associated P, mostly present as phosphate adsorbed to allophane and ferrihydrite. This suggests that the originally present apatite had to a large extent been weathered since the soils were formed after the last glaciation. The P speciation appeared to be strongly influenced by podzolization processes, where Al and Fe hydrous oxides, and allophane, are precipitated in the B horizon onto which the o-phosphate ions had been strongly adsorbed. The Al and Fe hydrous precipitates are present as coatings and in the pore spaces, which has been determining for the overall spatial distribution of P in the B horizon. In the Tärnsjö soil, there was a distinct difference as concerns the spatial heterogeneity of the P speciation between the upper 20 cm of the B horizon and the lower part. In the lower part there were smaller differences between individual spots in the relative proportions of the P species; Al-bound P always predominated over Fe-bound P (Table 2). In the uppermost part of the B horizon, however, Al-bound P predominated in some spots, while Fe-bound P predominated in others. A possible interpretation is that a large part of the secondary Al and Fe precipitates in the upper B horizon were formed and precipitated *in situ,* whereas in the deeper part of the B horizon, most of the Al and Fe precipitates were derived from Al and Fe that were mobilized in upper horizons and then translocated to the lower B horizon as organic complexes before being arrested and precipitated. Although a bit speculative, this interpretation is largely consistent with the prevailing ideas of the podzolization process (Lundström et al., 2000). In the Tönnersjöheden soil, however, there was no clear such trend.

A comparison of spot-wise μ-XANES results with those of bulk XANES showed a general consistency with respect to the dominant P species modelled by LCF, especially at the top soils of the two studied profiles. As expected, the higher resolution of P K-edge XANES spectroscopy that was acquired by the use of micro-focused beam shows greater diversity of P species than what was revealed by unfocused bulk soil XANES analysis. This is particularly evident in the better detection of organic P by the spot-wise μ-XANES when compared to that of the bulk XANES. For example, while LCF of bulk soil P XANES detected no organic P at Tärnsjö below 20 cm and at Tönnersjöheden below 40 cm depth, LCF of μ-XANES however estimated the presence of organic P to range from 5 to 16 and from 10 to 27% of total P at some microsites of these depths in Tärnsjö and Tönnersjöheden, respectively (Table 2 and 3). These μ-XANES results are further supported by the estimation of organic P in the ammonium oxalate soil extract, which shows that the proportion of total P in the form of organic P decreases with depth, ranging from 4 to 6% and from 8 to 19% in Tärnsjö 20–100 cm and Tönnersjöheden 40–100 cm, respectively (Fig. S17); at these depths organic P was not detectable by bulk XANES (Fig. 1). A similar loss of sensitivity concerning the detection of organic P species by bulk XANES when compared to spot-wise μ-XANES was previously reported by Hesterberg et al. (2017).

The largest differences between the spot-wise μ-XANES and bulk XANES was in the detection of Ca-bound P. While none of the upper soil horizon (0–50 cm) microsites studied by μ-XANES showed any presence of Ca-bound P, bulk P K-edge XANES showed Ca-bound P to increase with depth from 20 cm at the two sites, ranging from 10 to 50% and from 6 to 26% of total P in the 20–50 cm depths of Tärnsjö and Tönnersjöheden, respectively (Tables 2 and 3). This mismatch is not likely due to the lack of sensitivity in Ca-P detection by the μ-XANES considering the richness in unique futures of the XANES spectra for Ca phosphates when compared to other P species (Hesterberg, 2010) and the higher resolution of μ-XANES when compared to unfocused bulk P K-edge XANES (Hesterberg et al., 2017). Rather, our results suggest that, while Al-P, Fe-P and Org-P were localized at microsites that were < 200 μm apart, the Ca-bound P microsites were highly dispersed, probably > 600 μm apart, and were therefore for the most part not captured within the volume of soil mapped in our experiment. These results conform to the soil micro-chemical reactor concept suggested by Hesterberg et al. (2011), which states that 'each soil microsite represents an independent but interconnected micro-reactor of unique chemical composition'. Our results therefore further emphasize the significance of conceptualizing the soil fabric as networks of localized chemical micro-environments.

4.2. Implications for the influence of soil weathering on P speciation and cycling

Our results of multi-elemental imaging in combination with extraction data, μ-XANES and bulk XANES analysis suggest soil weathering and podzolization as major factors governing the abundance and availability of P in the studied forest soil profiles (Table 1, Fig. 1). Although it is difficult to clearly distinguish the P K-edge XANES spectra of lithogenic primary mineral apatite from those of precipitated or biogenically formed Ca-bound P (Hesterberg, 2010), previous studies of Ca-bound P formation and stability under different pH conditions showed formation of Ca-bound P to be unlikely under acidic soil conditions and the Ca-bound P detected in our study is therefore likely to be primary apatite (Eriksson et al., 2016; Nezat et al., 2008). Results from our study show apatite to occur as dispersed (several hundred μm apart) hot spots in the subsoils as inclusions in aluminosilicates or as discrete apatite grains, whereas the content of the apatite is absent or nearly absent in the upper soil horizons due to weathering. In the subsoil of Tönnersjöheden, appreciable amounts of apatite were identified, despite the relatively low pH (4.7–4.8). In Tärnsjö, such acidic conditions prevailed only in the uppermost horizons, where no apatite was identified. The reason why the Tönnersjöheden apatite has been preserved despite the low pH is not known. Possible reasons include a low surface area of the apatite, and that the pH of the soil at this site may only have been acidified in relatively recent times (Hallbäcken and Tamm, 1986). Our results are consistent with previous observations for soils of many temperate regions in which primary apatite was found to be absent or highly depleted in the upper 40 cm of the soils (Walker and Syers, 1976; Frossard et al., 1989; Werner et al., 2017a).

The primary apatite found in the lower B and C horizons represents a pool of P that trees can potentially acquire and thus add to the biogeochemically active P pool. As noted by Yanai et al. (2005) and Akselsson et al. (2008), this apatite may be important not only for the P nutrition but also for the availability (and leaching) of Ca, due to the very high weathering rate for apatite, particularly under acidic conditions. The μ-XANES data suggest that apatite is present both as inclusions in aluminosilicate minerals and as discrete mineral grains. The relative proportion of these phases is of considerable interest as the weathering rate of the latter is probably much higher, whereas apatite inclusions in feldspar were found to persist even in a strongly acidic E horizon of a Dutch Podzol (van Breemen et al., 2000). However, to quantify the relative importance of these phases, electron microscopy is possibly better suited than μ-XRF, because of the patch-wise distribution of apatite.

Lang et al. (2017) differentiated between relatively P-rich (often young) forest systems that "acquire" P and P-poor (often older) systems that "recycle" P. Clearly, due to the presence of apatite, it may be argued that our two soils are still acquiring P to some extent, although with time this apatite is likely to dissolve, causing the soils to approach "recycling" systems in the future. Further, Werner et al. (2017a) hypothesized that with increasing podzolisation, forest soils will increasingly recycle organic P whereas secondary Al and Fe precipitates will be dissolved because of the acid conditions and translocated downwards in the profile. According to the model of Werner et al. (2017a) our soils would be in an early stage of podzolisation. However, the B horizons of more northerly located forest ecosystems (such as our two soils) tend to have lower organic matter content at steady state than the systems studied by Werner et al. (2017a), due to lower mean annual temperature and lower N availability (Callesen et al., 2003; Olsson et al., 2009). Thus, the more advanced podzolisation stage, characterized by low pH and high organic matter content in the upper few decimetres of the soil, may therefore never be reached (unless the climate is changed). Despite this, it seems likely that when all reactive apatite is dissolved from the root zone, the P leaching from these northern Podzols is likely to become very low, due to the presence of non-crystalline Al and Fe precipitates that conserve P within the system and facilitate slow recycling. Therefore from a practical standpoint, such a system can be regarded as a "recycling" system, despite appreciable translocation within the profile and the predominance of inorganic P forms in the soil solid phase.

5. Conclusions

- For the first time, direct micro-spectroscopic data have been provided on spatially resolved chemical speciation of P in two Quaternary forest soil profiles.
- Microscale P heterogeneity in the forest soils was strongly influenced by soil weathering and pedogenesis.
- Due to soil acidity and weathering, lithogenic apatite had been depleted from the top soils, whereas in the C horizon, apatite appeared in hot spots either as inclusions in aluminosilicate minerals or as discrete mineral grains.
- Due to podzolisation, P was most abundant in the B horizons of the soil profiles, existing predominantly as P adsorbed to non-crystalline allophane and ferrihydrite, which were present as coatings on mineral grains and in pore spaces.
- Although the O horizon was dominated by organic P in both soils, the content of organic P was low in the mineral soil, not exceeding 25% of total P on average, although the organic P content was much higher in some microsites.

Declaration of Competing Interest

The authors declare that they have no known competing financial interests or personal relationships that could have appeared to influence the work reported in this paper.

Acknowledgments

This research was funded by the Swedish Research Council Formas, grant number 2017-01139, by the Geological Survey of Sweden, grant number 36-2044-2016, and by the Swedish Farmers' Foundation for Agricultural Research, grant number O-15-23-311.

We thank the Synchrotron Light Research Institute, Thailand and the SOLEIL synchrotron, France for providing beamtime through grant number 2012-3 and grant number 20180029, respectively. We thank Camille Rivard for the help with μXRF data processing. The support of the staff on beamline LUCIA, SLRI's BL8, XAS and laboratories at the

Swedish University of Agricultural Sciences is gratefully acknowledged.

Appendix A. Supplementary data

Supplementary data to this article can be found online at https://doi.org/10.1016/j.geoderma.2020.114550.

References

Akselsson, C., Westling, O., Alveteg, M., Thelin, G., Fransson, A.-M., Hellsten, S., 2008. The influence of N load and harvest intensity on the risk of P limitation in Swedish forest soils. Sci. Total Environ. 404 (2–3), 284–289.

Bain, D., Strand, L.T., Gustafsson, J., Melkerud, P.-A., Fraser, A., 2003. Chemistry, mineralogy and morphology of spodosols at two Swedish sites used to assess methods of counteracting acidification. Water Air Soil Pollut. Focus 3 (4), 29–47.

Baumann, K., Siebers, M., Kruse, J., Eckhardt, K.-U., Hu, Y., Michalik, D., Siebers, N., Kar, G., Karsten, U., Leinweber, P., 2019. Biological soil crusts as key player in biogeochemical P cycling during pedogenesis of sandy substrate. Geoderma 338, 145–158.

Beauchemin, S., Hesterberg, D., Chou, J., Beauchemin, M., Simard, R.R., Sayers, D.E., 2003. Speciation of phosphorus in phosphorus-enriched agricultural soils using X-ray absorption near-edge structure spectroscopy and chemical fractionation. J. Environ. Qual. 32 (5), 1809–1819.

Binkley, D., Högberg, P., 2016. Tamm review: revisiting the influence of nitrogen deposition on Swedish forests. For. Ecol. Manage. 368, 222–239.

Callesen, I., Liski, J., Raulund-Rasmussen, K., Olsson, M., Tau-Strand, L., Vesterdal, L., Westman, C., 2003. Soil carbon stores in Nordic well-drained forest soils—Relationships with climate and texture class. Glob. Change Biol. 9 (3), 358–370.

Church, C., Spargo, J., Fishel, S., 2017. Strong acid extraction methods for "total phosphorus" in soils: EPA Method 3050B and EPA Method 3051. Agric. Environ. Lett. 2 (1), 1–3.

Cordell, D., Drangert, J.-O., White, S., 2009. The story of phosphorus: global food security and food for thought. Global Environ. Change 19 (2), 292–305.

Eriksson, A.K., Hillier, S., Hesterberg, D., Klysubun, W., Ulén, B., Gustafsson, J.P., 2016. Evolution of phosphorus speciation with depth in an agricultural soil profile. Geoderma 280, 29–37.

Frossard, E., Stewart, J.W.B., St., Arnaud, R.J., 1989. Distribution and mobility of phosphorus in grassland and forest soils of Saskatchewan. Can. J. Soil Sci. 69, 401–416.

Frossard, E., Condron, L.M., Oberson, A., Sinaj, S., Fardeau, J., 2000. Processes governing phosphorus availability in temperate soils. J. Environ. Qual. 29 (1), 15–23.

Gundersen, P., Schmidt, I.K., Raulund-Rasmussen, K., 2006. Leaching of nitrate from temperate forests effects of air pollution and forest management. Environ. Rev. 14 (1), 1–57.

Gustafsson, J.P., Braun, S., Tuyishime, J.M.R., Adediran, G., Warrinnier, R., Hesterberg, D., 2020. A probabilistic approach to phosphorus speciation of soils using P K-edge XANES spectroscopy with linear combination fitting. Soil Systems 4 (26).

Gustafsson, J.P., Akram, M., Tiberg, C., 2015. Predicting sulphate adsorption/desorption in forest soils: evaluation of an extended Freundlich equation. Chemosphere 119, 83–89.

Gustafsson, J.P., Bhattacharya, P., Karltun, E., 1999. Mineralogy of poorly crystalline aluminium phases in the B horizon of Podzols in southern Sweden. Appl. Geochem. 14 (6), 707–718.

Hallbäcken, L., Tamm, C.O., 1986. Changes in soil acidity from 1927 to 1982–1984 in a forest area of south-west Sweden. Scand. J. For. Res. 1 (1–4), 219–232.

Hansson, K., Olsson, B.A., Olsson, M., Johansson, U., Kleja, D.B., 2011. Differences in soil properties in adjacent stands of Scots pine, Norway spruce and silver birch in SW Sweden. For. Ecol. Manage. 262 (3), 522–530.

Heindel, R.C., Lyons, W.B., Welch, S.A., Spickard, A.M., Virginia, R.A., 2018. Biogeochemical weathering of soil apatite grains in the McMurdo Dry Valleys, Antarctica. Geoderma 320, 136–145.

Hesterberg, D., 2010. Macroscale chemical properties and X-ray absorption spectroscopy of soil phosphorus, Developments in Soil Science. Elsevier 313–356.

Hesterberg, D., Duff, M.C., Dixon, J.B., Vepraskas, M.J., 2011. X-ray microspectroscopy and chemical reactions in soil microsites. J. Environ. Qual. 40 (3), 667–678.

Hesterberg, D., McNulty, I., Thieme, J., 2017. Speciation of soil phosphorus assessed by XANES spectroscopy at different spatial scales. J. Environ. Qual. 46 (6), 1190–1197.

Hesterberg, D., Zhou, W., Hutchison, K., Beauchemin, S., Sayers, D., 1999. XAFS study of adsorbed and mineral forms of phosphate. J. Synchrotron Radiat. 6 (3), 636–638.

IUSS Working Group WRB, 2014. World reference base for soil resources 2014. International soil classification system for naming soils and creating legends for soil maps. World Soil Resources Reports No. 106. FAO, Rome.

Klysubun, W., Tarawarakarn, P., Thamsanong, N., Amonpattaratkit, P., Cholsuk, C., Lapboonrueng, S., Chaichuay, S., Wongtepa, W., 2020. Upgrade of SLRI BL8 beamline for XAFS spectroscopy in a photon energy range of 1–13 keV. Radiat. Phys. Chem. 175, 108145.

Lang, F., Krüger, J., Amelung, W., Willbold, S., Frossard, E., Bünemann, E.K., Bauhus, J., Nitschke, R., Kandeler, E., Marhan, S., 2017. Soil phosphorus supply controls P nutrition strategies of beech forest ecosystems in Central Europe. Biogeochemistry 136 (1), 5–29.

Lundström, U.S., van Breemen, N., Bain, D., 2000. The podzolization process. A review. Geoderma 94 (2–4), 91–107.

Nezat, C.A., Blum, J.D., Yanai, R.D., Park, B.B., 2008. Mineral sources of calcium and phosphorus in soils of the northeastern United States. Soil Sci. Soc. Am. J. 72 (6), 1786–1794.

Olsson, M.T., Erlandsson, M., Lundin, L., Nilsson, T., Nilsson, Å., Stendahl, J., 2009. Organic carbon stocks in Swedish Podzol soils in relation to soil hydrology and other site characteristics. Silva Fennica 43 (2), 209–222.

Prietzel, J., Klysubun, W., Werner, F., 2016. Speciation of phosphorus in temperate zone forest soils as assessed by combined wet-chemical fractionation and XANES spectroscopy. J. Plant Nutr. Soil Sci. 179 (2), 168–185.

Ravel, B., Newville, M., 2005. ATHENA, ARTEMIS, HEPHAESTUS: data analysis for X-ray absorption spectroscopy using IFEFFIT. J. Synchrot. Radiation 12 (4), 537–541.

Rivard, C., Lanson, B., Cotte, M., 2016. Phosphorus speciation and micro-scale spatial distribution in North-American temperate agricultural soils from micro X-ray fluorescence and X-ray absorption near-edge spectroscopy. Plant Soil 401 (1–2), 7–22.

Smits, M.M., Johansson, L., Wallander, H., 2014. Soil fungi appear to have a retarding rather than a stimulating role on soil apatite weathering. Plant Soil 385 (1–2), 217–228.

Solé, V., Papillon, E., Cotte, M., Walter, P., Susini, J., 2007. A multiplatform code for the analysis of energy-dispersive X-ray fluorescence spectra. Spectrochim. Acta, Part B 62 (1), 63–68.

Syers, J., Williams, J., Campbell, A., Walker, T., 1967. The significance of apatite inclusions in soil phosphorus studies. Soil Sci. Soc. Am. J. 31 (6), 752–756.

Tannazi, F., Bunker, G., 2005. Determination of chemical speciation by XAFS. Phys. Scr. 2005 (T115), 953.

Van Breemen, N., Finlay, R., Lundström, U., Jongmans, A.G., Giesler, R., Olsson, M., 2000. Mycorrhizal weathering: a true case of mineral plant nutrition? Biogeochemistry 49 (1), 53–67.

Van Reeuwijk, L., 1995. Procedures for soil analyses. International Soil Reference and Information Centre, Wageningen, Netherlands.

Van Vuuren, D.P., Bouwman, A.F., Beusen, A.H., 2010. Phosphorus demand for the 1970–2100 period: a scenario analysis of resource depletion. Global Environ. Change 20 (3), 428–439.

Vantelon, D., Trcera, N., Roy, D., Moreno, T., Mailly, D., Guilet, S., Metchalkov, E., Delmotte, F., Lassalle, B., Lagarde, P., 2016. The LUCIA beamline at SOLEIL. J. Synchrotron Radiat. 23 (2), 635–640.

Vincent, A.G., Schleucher, J., Gröbner, G., Vestergren, J., Persson, P., Jansson, M., Giesler, R., 2012. Changes in organic phosphorus composition in boreal forest humus soils: the role of iron and aluminium. Biogeochemistry 108 (1–3), 485–499.

Walker, T., Syers, J.K., 1976. The fate of phosphorus during pedogenesis. Geoderma 15 (1), 1–19.

Wallander, H., Wickman, T., Jacks, G., 1997. Apatite as a P source in mycorrhizal and non-mycorrhizal Pinus sylvestris seedlings. Plant Soil 196 (1), 123–131.

Werner, F., de la Haye, T.R., Spielvogel, S., Prietzel, J., 2017a. Small-scale spatial distribution of phosphorus fractions in soils from silicate parent material with different degree of podzolization. Geoderma 302, 52–65.

Werner, F., Mueller, C.W., Thieme, J., Gianoncelli, A., Rivard, C., Höschen, C., Prietzel, J., 2017b. Micro-scale heterogeneity of soil phosphorus depends on soil substrate and depth. Sci. Rep. 7 (1), 3203.

Wolf, A., Baker, D., 1990. Colorimetric method for phosphorus measurement in ammonium oxalate soil extracts. Commun. Soil Sci. Plant Anal. 21 (19–20), 2257–2263.

Yanai, R.D., Blum, J.D., Hamburg, S.P., Arthur, M.A., Nezat, C.A., Siccama, T.G., 2005. New insights into calcium depletion in northeastern forests. J. Forest. 103 (1), 14–20.

Yu, L., Zanchi, G., Akselsson, C., Wallander, H., Belyazid, S., 2018. Modeling the forest phosphorus nutrition in a southwestern Swedish forest site. Ecol. Model. 369, 88–100.

Zetterberg, T., Olsson, B.A., Löfgren, S., von Brömssen, C., Brandtberg, P.-O., 2013. The effect of harvest intensity on long-term calcium dynamics in soil and soil solution at three coniferous sites in Sweden. For. Ecol. Manage. 302, 280–294.